32nd URSI GASS, Montreal, 19–26 August 2017

Transistor-Loaded Isolator Based on both Frustrated Propagation and Field Cancellation Mechanisms

Yuhi Yokohama*, Toshiro Kodera
Department of Interdisciplinary Science and Engineering, Meisei University, Tokyo, 1918506, Japan

Abstract

A novel microwave isolator operation based on non-reciprocal vectorial magnetic field cancellation in Magnet-less non-reciprocal Metamaterial (MNM) is proposed, analyzed, and its superiority to the previous concept is fully confirmed by prototype device. The field cancellation is realized by a traveling-wave ring resonator pair with structural perturbation in order to obtain asymmetric vectorial field excitation, which leads to vectorial field cancellation. Compared to the original design, isolation ratio ($|S_{21}| - |S_{12}|$) is improved from 10 to 35 dB with insertion loss of 2 dB.

1 Introduction

Magnet-less Non-reciprocal Metamaterial (MNM) [1, 2, 3] was presented as an counterpart to biased ferrite[4]. MNM is an artificial electromagnetic metamaterial technology mimicking magnetic gyrotropic properties, and various non-reciprocal microwave devices can be realized in the same manner of conventional microwave ferrite devices[3] without any iron-oxide material but purely consisting of integrated circuit compatible materials. In this paper, novel isolator operation using vectorial field cancellation in MNM is proposed. The measurement results indicates the feasibility of field cancelling mode, providing *zero magnetic field area*. Currently the verification is limited to planar isolator but also useful for novel artificial electromagnetic boundary.

2 Principle of Operation

Figure 1 shows the principle of operation in microwave isolator utilizing the artificial magnetic gyrotropy induced by MNM[3]. This structure consists of two layers, FET inserted metal ring pair on dielectric and microstrip line (MSL) on dielectric above it. The propagating wave along MSL consequently excite rotating magnetic field even without ring, where its rotation direction are CW on left side and CCW on right side toward propagation[5]. The forward (transmission direction) case, traveling-wave resonance arises in FET inserted ring resonator pair through electromagnetic coupling to MSL according to same directionally rotating magnetic field. The reverse transmission

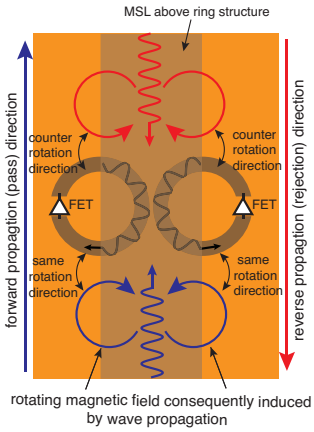

Figure 1. Principle of microwave isolator utilizing magnetic gyrotropy induced by MNM structure.

(rejection) case, rotating field in MSL has a opposite direction to that defined by unilateral FET property. Electromagnetic field is excited by coupling but the rotating magnetic field excited in ring does not contribute to wave propagation, therefore isolator operation is obtained. Figure 2

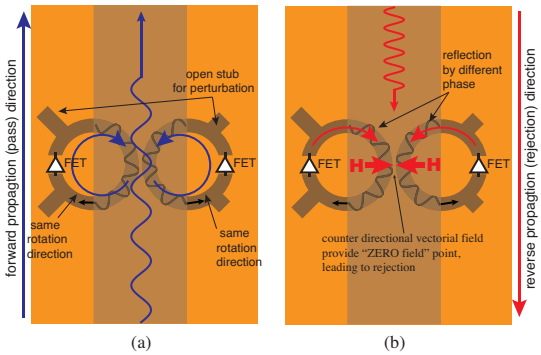

Figure 2. Proposed improved isolator operation based on asymmetrically perturbed resonant ring pair. (a) Forward propagation case. (b) Reverse propagation case.

shows the improved microwave isolator operation based on MNM, with asymmetry perturbed resonant ring pair by different length open stub. In the forward propagation case, the rotating magnetic field in MSL directs to the direction of the field in metal ring defined by FET insertion, therefore the excited field in the ring pair contribute to wave propa-

gation as same as in fig.1.

In the reverse propagation case, counter-directional rotation field excited in rings does not contribute to wave propagation, and the excited field on the rings have different phase property by asymmetric structure. When two rings have in-phase oscillation, the field between ring is totally canceled out. In this paper, four stub lengths are optimized to in-phase oscillation by parametric study in commercial simulator (*CST microwave studio*). Fig. 3 shows the pro-

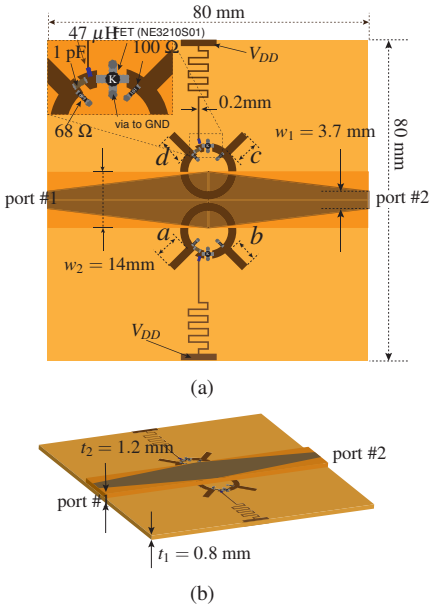

Figure 3. Structure of the proposed isolator. (a) Top view. (b) Perspective view.

posed isolator structure, consisting of two layers (FET inserted metal ring pair on dielectric, and MSL on dielectric above). Top layer has 0.4 mm thick, and its total is 1.2 mm. Top MSL is linearly tapered for smooth impedance matching to 50Ω. The bias voltages for FETs (NE3210S01) are feed through meander lines and chip inductors (47nH). Ohmic resistors (100Ω and 68Ω) are inserted for impedance matching between FET and ring resonator. Ohmic matching is not ideal in view point of power consumption, but these are employed due to footprint limitation within resonant particle. Each ring has two open stubs arranged in 90° position. Length of open stubs are defined by a to d, as illustrated in figure.

3 Simulation results

The transmission characteristics and field profile of fig. 3 are simulated by commercial simulator *CST Microwave Studio*. FET part is simulated by 50Ω matched ideal isolator block. Figure 4 shows the results of transmission characteristics for non-perturbed symmetric ring pair ($a = b = c = d = 0$). Isolation ($|S_{21}| - |S_{12}|$) is 13 dB at 2.82 GHz.

Figure 5 shows vectorial magnetic field profile at middle of lower dielectric layer (0.4 mm from bottom) for the

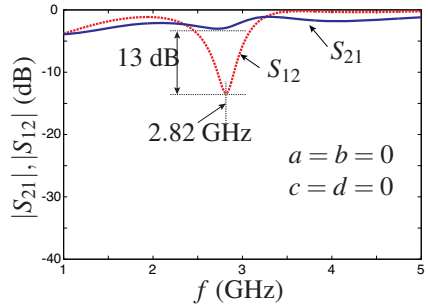

Figure 4. Simulation results of transmission characteristics for non-perturbed symmetric ring pair ($a = b = c = d = 0$). Isolation ($|S_{21}| - |S_{12}|$) is 13 dB at 2.82 GHz.

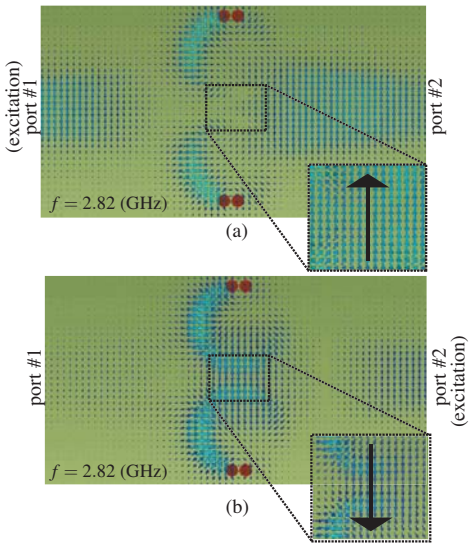

Figure 5. Vectorial magnetic field profile at middle of lower dielectric layer (0.4 mm from bottom) for the maximum isolation frequency (2.82 GHz) in fig.4. (a) Forward transmission case. (b) Reverse transmission case.

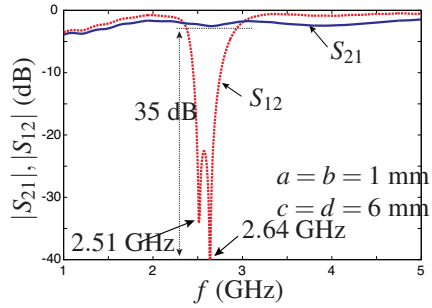

Figure 6. Simulation results of transmission characteristics for perturbed asymmetric ring pair ($a = b = 1, c = d = 6$ mm).

maximum isolation frequency (2.82 GHz) in fig.4. Insets plot enlarged field between rings. Fig. 5 (a) shows the forward transmission case, where vectorial fields are totally aligned. Fig. 5 (b) shows the reverse transmission case, where vectorial fields are aligned. These vectors oscillate in harmonic regime. Figure 6 shows the simulation results of transmission characteristics for perturbed asymmetric ring pair ($a = b = 1, c = d = 6$ mm). These stub parameters are optimized by simulator to obtain maximum isolation with lower insertion loss. Compared to non-perturbed case, isolation is greatly improved from 13 dB to 35 dB. Due to the structural asymmetry, each ring naturally has different resonant frequency, and electromagnetic coupling provides split dip response for $|S_{12}|$. For the dip frequency of 2.51 GHz and 2.64 GHz, field profile is examined. Figure 7 shows the

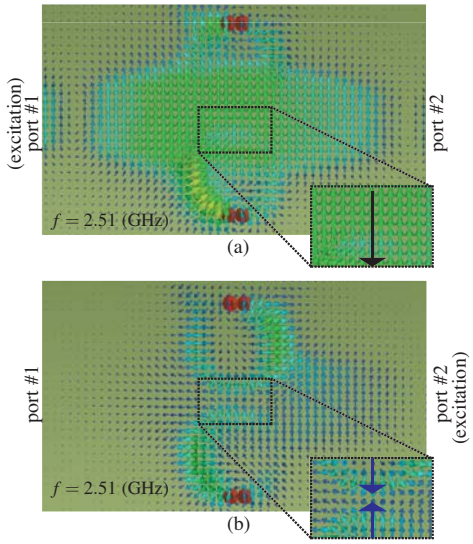

Figure 7. Vectorial magnetic field profile at middle of lower dielectric layer (0.4 mm from bottom) for the lower dip frequency (2.51 GHz) in fig.6. Insets plot enlarged field between rings. (a) Forward transmission case(b) Reverse transmission case.

vectorial magnetic field profile at middle of lower dielectric layer (0.4 mm from bottom) for the lower dip frequency (2.51 GHz) in fig.6. Fig. 7(a) shows forward transmission case, where vectorial fields are aligned and rotating magnetic field in each rings contribute to wave propagation. Fig. 7(b) shows the reverse transmission case, where vectorial field in upper and bottom ring are *counter directional* organizing "*zero magnetic field area*". The propagating wave in MSL has a maximum magnetic field in the centre and this field vacancy leads to transmission rejection. Figure 8 shows the vectorial magnetic field profile at middle of lower dielectric layer (0.4 mm from bottom) for the higher dip frequency (2.64 GHz) in fig.6. The forward case does not show significant difference, but the reverse case, field profile is completely different to fig.7. The vectorial field in upper and bottom ring are aligned as same manner as non-perturbed reverse propagation case in fig.5, and field cancellation does not appear. Figures 7 and 8 clearly show the two dips in fig. 6 appears by different phenomena.

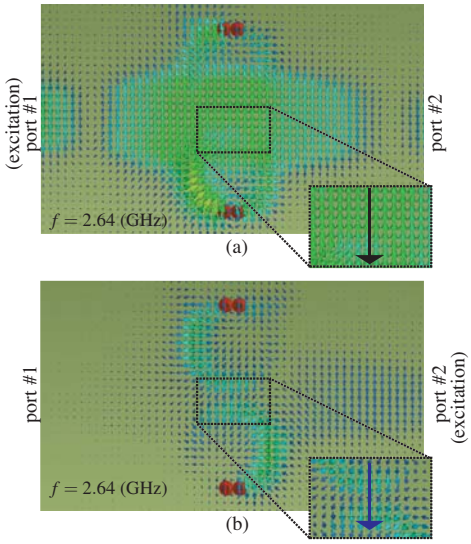

Figure 8. Vectorial magnetic field profile at middle of lower dielectric layer (0.4 mm from bottom) for the higher dip frequency (2.64 GHz) in fig.6. (a) Forward transmission case. (b) Reverse transmission case.

4 Measurement results

In order to confirm the feasibility of the simulation response, two prototypes (no open stub and with stubs by optimized values) are made and its characteristics are investigated. Figure 9 shows the prototype for $a = b = c = d = 0$ (no stub) case and its measured values are shown in Fig. 10. As expected in fig.4, isolation is limited to 12 dB at 2.94 GHz. The response as an isolator is not so significant but total response has a very good agreement to simulation result of fig. 4, which indicates the validity of modeling by simulation.

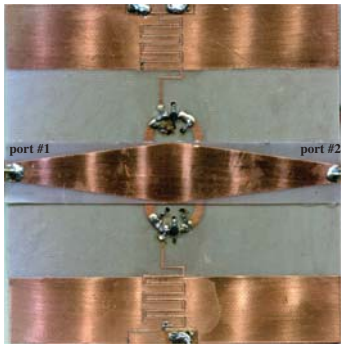

Figure 9. Prototype device without stub structure ($a = b = c = d = 0$).

Figure 11 shows the prototype device with asymmetric stub structure ($a = b = 1$, $c = d = 6$ mm), corresponding to the structure giving fig.6, and its measured transmission characteristics is shown in Fig. 13. As expected in fig.6, isolation is greatly improved compared to fig. 10, and split-dip response is observed at 2.49 GHz and 2.81 GHz and its isolation is highly improved to 52 dB at 2.81 GHz. The

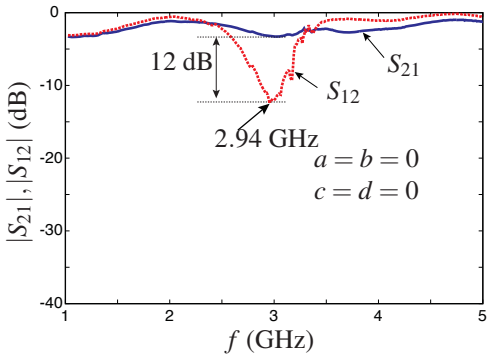

Figure 10. Measured transmission characteristics for the device in fig.9.

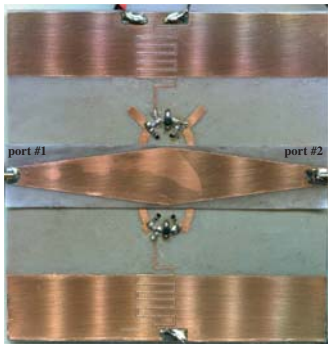

Figure 11. Prototype device with asymmetric stub structure ($a = b = 1$, $c = d = 6$ mm), corresponding to the structure giving the response of fig.6.

Figure 12. One unit FET in the ring resonators of the isolator in Fig. 11 for isolation comparison.

field profile cannot be prospected by transmission, but these two dips can be expected to correspond to the new isolator mode, “field cancelling", and the previously reported operation. In addition, the realised isolation well excesses that of FET alone, whose response is obtained by the device in fig. 12. The combination of electromagnetic effect by structure and unilaterality of FET provides super performance to that of single FET.

5 Concludion

Novel isolator operation using vectorial field cancellation in Magnet-less Non-Reciprocal Metamaterial (MNM) is examined numerically and experimentally. The measurement results indicates the feasibility of field cancelling mode, providing *zero magnetic field area*. Currently the verification is limited to planar isolator but also useful for novel

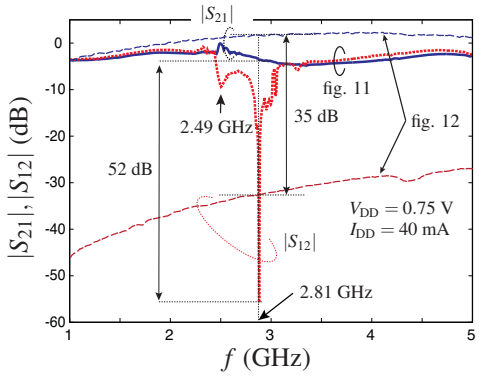

Figure 13. Measured transmission characteristics for the device in fig.11 and 12. As expected in fig.6, split-dip response is observed at 2.49 GHz and 2.81 GHz and its isolation is significantly improved to 52 dB at 2.81 GHz.

artificial electromagnetic boundary.

6 Acknowledgements

This work has been carried out under the sponsorship of KAKENHI Grant-in-Aid for Research Activity # 26289106.

References

[1] T. Kodera, D. L. Sounas, and C. Caloz, “Artificial Faraday rotation using a ring metamaterial structure without static magnetic field," *Appl. Phys. Lett.*, vol. 99, pp. 031114:1-3, July 2011.

[2] D. L. Sounas, T. Kodera, and C. Caloz, “Electromagnetic Modeling of a Magnetless Nonreciprocal Gyrotropic Metasurface", IEEE Trans. AP, Vol. 61, No. 1, pp. 221-231, Jan. 2013.

[3] T. Kodera, D. L. Sounas, and C. Caloz,“Magnetless Noreciprocal Metamaterial (MNM) Technology: Application to Microwave Components", IEEE Trans. MTT, Vol. 61, No. 3, pp. 1030-1042, Mar 2013.

[4] B. Lax and K. J. Button, *Microwave Ferrites and Ferrimagnetics*, McGraw-Hill, 1962.

[5] J. Adam, L. Davis, G. Dionne, E. Schloemann, and S. Stizer, “Ferrite devices and materials," *IEEE Trans. Microwave Theory Tech.*, vol. 50, no. 3, pp. 721–737, March 2002.